Weight functions for opening mode stress intensity factors for double edge cracked rings using two reference configurations

Mohammed Shafeeque K K*, K V N Surendra

Indian Institute of Technology Palakkad, Kanjikode, Palakkad, 678623, Kerala, India

Abstract

Weight functions (WF) to determine the opening mode stress intensity factors (SIFs) of both inner and outer double edge cracked ring specimens are derived. Various WF forms available in the literature and two new forms are considered to arrive at the optimum form for WF of the cracked-ring specimens. The method in which only two reference loading configurations are required, is adopted for deriving the WF. Uniform and linear crack face pressures are used as the two loading configurations for which SIFs are obtained using the finite element method (FEM). An investigation is done to find the accurate WF among various forms by comparing their SIF predictions with those by FEM. The comparison shows that the dual form factor method of WF leads to accurate results for the two ring specimens with less than 1% error. The finally arrived WF is then applied to determine the SIFs of the inner as well as outer double edge cracked circular rings for various inner to outer radii subjected to diametral compression on the outer boundary.

Keywords: Weight function, stress intensity factor, linear elastic fracture mechanics, uniform crack face pressure, linear crack face pressure, uniform compression.

*Corresponding author

Email address: kkmshafeeque@gmail.com (Mohammed Shafeeque K K)

Preprint submitted to Elsevier *January 23, 2025*

1. Introduction

Compressive test specimens are widely used for fracture studies of brittle materials like rocks, concrete, ceramics, glasses for which the linear elastic fracture mechanics (LEFM) can be applied. The stress intensity factor (SIF), formulated in LEFM, characterizes the singular stress and strain fields near the tip of the crack. The critical value of SIF for a given material is taken as its fracture toughness. The determination of SIF and fracture toughness is an essential task in the damage-tolerant design philosophy and the predictions of the growth life of crack fatigue. Cracked circular ring specimens have been used for compressive as well as tensile fracture testing for pure mode-I, mode-II, and mixed mode I-II fracture behavior of different materials. Numerous works can be found on cracked circular ring specimens for fracture studies of different materials. For example, fracture toughness of Aluminium and Uranium alloy was determined by using finite element method (FEM) and experiments on cracked circular rings by Jones [?]. The mixed mode I-II fracture toughness of anisotropic rocks employing circular ring specimens was found by Chen et al. [?]. Ahmad and Ashbaugh [?] investigated a single edge cracked circular ring specimen to design a constant K_I specimen for a wide range of crack lengths using FEM.

A circular ring specimen can also be used to study the unstable crack propagation and crack arrest behaviour of different materials. Iung and Pineau [?] investigated this aspect of the ring specimen using finite element code for static analysis and using ABAQUS software for elasto-dynamic analysis. The investigations on the circular ring specimen were carried out using various techniques by different researchers. For example, Bowie and Freese [?] using the boundary collocation method, Tracy [?] using modified collocation technique and partitioning, Leung and Hu [?] using the dislocation solution and the singular integral equation technique, Murukami et al. [?] using the body force method and Chen et al. [?] using the boundary element method analysed the cracked ring specimens for different modes of fracture.

The weight function (WF) method, first proposed by Bueckner [?] and then by Rice [?], is a powerful technique in fracture mechanics to determine the SIF in a given cracked solid. The mode-I stress intensity factors (K_I) for cracked rings of inner to outer radii ratios (R_i/R_o) of 0.5 and 0.8, subjected to arbitrary crack face pressure were obtained by using WF technique by Grandt [?]. Petroski and Achenbach [?] also obtained the same results for a circular ring of $R_i/R_o = 0.5$. Graham [?] also used WF to determine the K_I for a thick cylinder of $R_i/R_o = 0.55$. Then, Andrasic and Parker [?] determined K_I for a wide range of thick cylinders. Sha and Yang [?] and Ma et al. [?] used WF technique to find the K_I for cracked hollow disks and cylinders.

In all these works, WF is derived for cracked rings for a particular value of R_i/R_o and is determined based on crack opening displacements (COD) from a reference configuration. The main shortcoming of this approach to derive WF is that CODs may not be accurate and are heavily dependent on the loading configuration, which leads to significant error in SIF predictions when using such WF for the other loading configurations. This can be overcome by using WF from multiple reference configurations. Weight function for a double edge cracked circular ring using the method of multiple reference configuration is not available in the literature, although COD-based WFs were reported for the double edge cracked ring [? ?]. This paper uses various forms of WF available in the literature and some novel forms, and utilizes multiple reference configurations, to derive and investigate the precision of the WFs for inner/outer double edge cracked circular ring specimens as in Fig. 1 for various R_i/R_o. The derived WFs are then used to find the K_I for two loading conditions to compare the results with the FEM results to test the accuracy.

The theory behind the WF for K_I evaluation is reviewed in Section 2. The weight functions for K_I of the two cracked rings are formulated in Section 3. The validation of the derived WFs for SIFs and their application to determine the K_I of the inner/outer cracked ring specimens of different R_i/R_o, subjected to diametral compression, are given in Section 5. The last Section 6 concludes our work.

2. Weight function method

According to the WF method, the SIF of a cracked solid can be determined for any loading condition by knowing the WF and the stresses along the prospective crack in the uncracked solid. The weight function method, along with the superposition principle in LEFM, offers an efficient method to determine the SIF of any given cracked solid. Using the definition of WF, the mode-I stress intensity factor (K_I) is expressed as in Eq. (1) [?].

$$K_I = \int_0^a \sigma_{yy}(x) W(x, a) dx \tag{1}$$

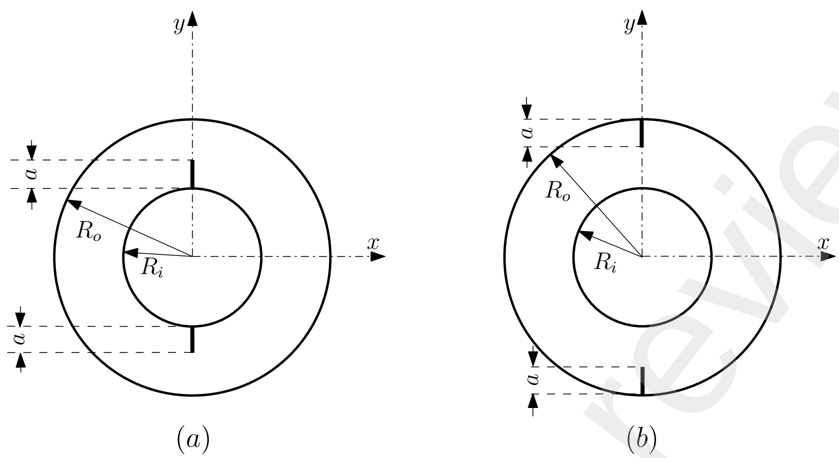

ht

Figure 1: Circular ring specimen geometries:(a) inner double edge cracked (b) outer double edge cracked

where, $\sigma_{yy}(x)$ is the Cartesian opening stress component in the uncracked body, a is the crack-length and $W(x, a)$ is the weight function for the mode-I SIF.

The stresses in the uncracked body can be obtained by analytical or numerical methods for stress analysis in elasticity. For determining the WF, various methods are available in the literature. Bueckner [**?**] and Rice [**?**] introduced the displacement-based WF by relating WF with the crack opening displacement (COD) for a reference loading configuration as given in Eq. (2).

$$W(x, a) = \frac{E'}{K_{Ir}} . \frac{\partial u_r(x, a)}{\partial a} \tag{2}$$

where, E' is the effective modulus (E for plane stress and $E/(1-\nu^2)$ for plane strain), K_{Ir} is the mode-I SIF and u_r is the COD for a reference configuration.

Fett et al. [**?**] proposed a general WF in the form of a series expression as in Eq. (3).

$$W(x, a) = \frac{2}{\sqrt{[2\pi(a-x)]}} \left[1 + \sum_{1}^{n} m_i \left(1 - x/a\right)^n \right] \tag{3}$$

Sha & Yang [**?**] also suggested another expression of WF, which was also in series form as in Eq. (4).

$$W(x,a) = \frac{2}{\sqrt{[2\pi(a-x)]}}\left[1+\sum_{1}^{n} m_i\left(1-x/a\right)^{n/2}\right] \tag{4}$$

The different mathematical representations of the WF correspond to particular crack geometries and mathematical approaches. However, Glinka and Shen [**?**] stated that several existing WFs for various geometries of cracked solids have the same singular term which may be accurately approximated to a general expression of WFs, known as Universal WF form, as expressed in Eq. (5).

$$\begin{aligned} W(x,a) = \frac{2}{\sqrt{2\pi(a-x)}}\Bigg[1 + m_1\left(1-\frac{x}{a}\right)^{1/2} + m_2\left(1-\frac{x}{a}\right) \\ + m_3\left(1-\frac{x}{a}\right)^{3/2}\Bigg] \end{aligned} \tag{5}$$

The unknown parameters m_1, m_2 and m_3 can be determined by using solutions from reference configurations. To determine these parameters, the method of three reference SIFs or the method of two reference SIFs can be used.

In this work, a new form of WF as in Eq. (6) *(WF Form-3)* is also considered which is comparable in form to the universal WF form.

$$\begin{aligned} W(x,a) = \frac{2}{\sqrt{\pi a}}\Bigg[\left(1-\frac{x}{a}\right)^{-1/2} + m_1\left(1-\frac{x}{a}\right)^{1/2} + m_2\left(1-\frac{x}{a}\right)^{3/2} \\ + m_3\left(1-\frac{x}{a}\right)\Bigg] \end{aligned} \tag{6}$$

Two other alternative forms to WF Form-3 (Eq. (6)) with the exponents of the four terms {-1/2, 1/2, 1, 2} and {-1/2, 1/2, 3/2, 0} in place of {-1/2, 1/2, 3/21}, is tested for accuracy, and found that the alternatives will not lead to enough accurate results.

Another way to synthesize weight functions for cracked bodies is using the dual form factor (DFF) method. In this method, it solves a set of dual integral equations that relates the form factors, the weight function, and the normal stress distributions on the crack line for the two reference loading configurations [**?**]. In this case, the expression for WF as in Eq. (7) *(WF-DFF)* is taken and the unknown coefficients m_1 and m_2 are determined from two reference loading configurations.

$$W(x,a) = \sqrt{\frac{2}{\pi a}} \left[\left(1 - \frac{x}{a}\right)^{-1/2} + m_1 \left(1 - \frac{x}{a}\right)^{1/2} + m_2 \left(1 - \frac{x}{a}\right)^{3/2} \right] \quad (7)$$

Considering different combinations of the exponents of the three terms in the above WF form of DFF (viz. $\{-1/2, 1/2, 1\}$, $\{-1/2, 1, 3/2\}$, $\{1/2, 1, 3/2\}$), the best combination ($\{-1/2, 1/2, 1\}$) is chosen for further analysis and comparison against other standard forms. We call this form *WF-DFF Form-2*, is given in Eq. (8).

$$W(x,a) = \sqrt{\frac{2}{\pi a}} \left[\left(1 - \frac{x}{a}\right)^{-1/2} + m_1 \left(1 - \frac{x}{a}\right)^{1/2} + m_2 \left(1 - \frac{x}{a}\right) \right] \quad (8)$$

3. Weight function formulations for Double edge cracked circular rings

Weight functions for the double-edge cracked circular ring specimens are derived here using the method of two reference SIFs, in which two different loading configurations are used as reference. The uniform pressure distribution and linear pressure distribution on the crack faces are taken here as the two reference configurations for the specimens of inner and outer double edge cracked circular rings, as shown in Figs. 2 & 3 respectively.

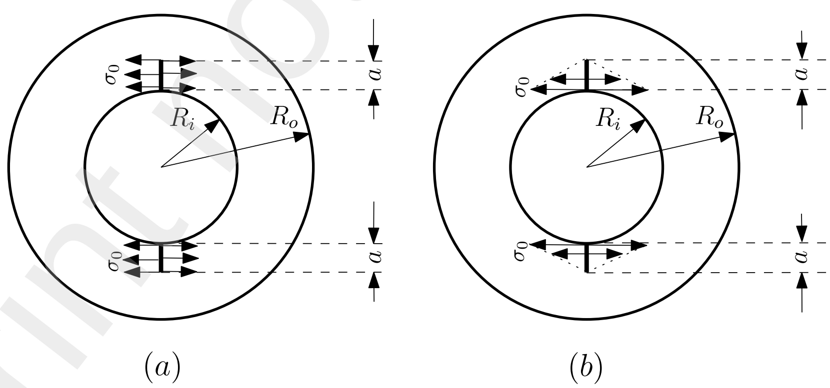

Figure 2: Inner double edge cracked Circular ring under crack-face pressure: (a) Uniform distribution of pressure (b) Linear distribution of pressure.

The first reference configuration of uniform pressure distribution of magnitude ($\sigma_{yy}^{(r1)}(x) = \sigma_0$) on the crack face as shown in Fig. 2(a) & 3(a). The

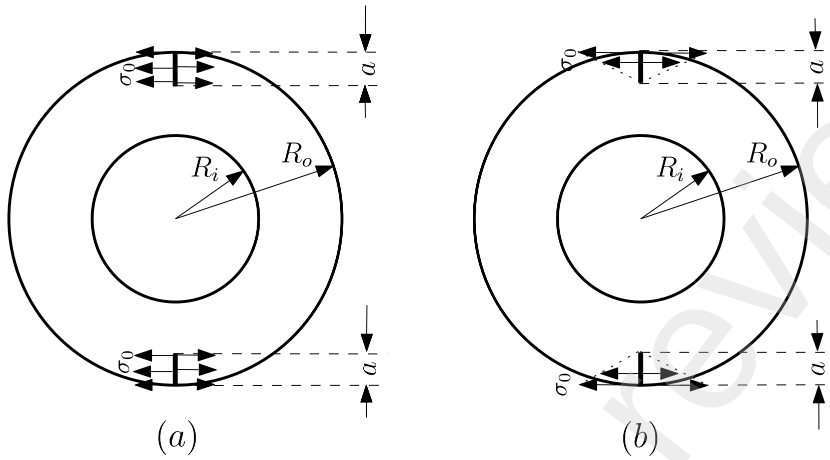

Figure 3: Outer double edge cracked Circular rings: (a) Uniform crack-face pressure and (b) Linearly distributed crack-face pressure.

mode-I stress intensity factor developed at the crack-tip of the circular ring ($K_I^{(r1)}$) and the corresponding normalized stress intensity factor or the form factor ($F_I^{(r1)}$) ((F_I defined later in Eq. (27)), can be derived using the definition of WF for SIF as in Eq. (1) and the various forms of WF as explained in the above section (Eqs. (3), (5), (6), (7) & (8)) for the uniform crack face pressure case. The second loading configuration is taken as $\sigma_{yy}^{(r2)}(x) = \sigma_0(1-x/a)$ where x is measured from the crack mouth, on the crack face (linearly varying pressure load) which is shown in Fig. 2(b) & 3(b). The mode-I SIF ($K_I^{(r2)}$) and the corresponding form factor ($F_I^{(r2)}$) can also be derived for the linear crack face pressure using Eq. (1). The weight function formulations for the cracked circular rings using various WF forms mentioned in the above section are briefly described below.

3.1. General WF form by Fett

A truncated form of general WF form by Fett (Eq. (3)) is used here with three terms of unknown coefficients m_1, m_2 & m_3. The three coefficients can be find from three equations, in which two equations are derived by connecting the reference mode-I SIFs, $K_I^{(r1)}$ and $K_I^{(r1)}$, to the WF equations. The additional equation is from the characteristic property of WF at the crack mouth (at $x = 0$), which is obtained from the slope of crack opening displacement at the crack mouth, which was noted by Fett [**?**].

$$K_I^{(r1)} = \sigma_0\sqrt{\pi a}F_I^{(r1)} = \int_0^a \sigma_{yy}^{r1}(x)\frac{2}{\sqrt{2\pi(a-x)}}\left[1 + m_1\left(1-\frac{x}{a}\right) + m_2\left(1-\frac{x}{a}\right)^2 + m_3\left(1-\frac{x}{a}\right)^3\right]dx \quad (9)$$

$$K_I^{(r2)} = \sigma_0\sqrt{\pi a}F_I^{(r2)} = \int_0^a \sigma_{yy}^{r2}(x)\frac{2}{\sqrt{2\pi(a-x)}}\left[1 + m_1\left(1-\frac{x}{a}\right) + m_2\left(1-\frac{x}{a}\right)^2 + m_3\left(1-\frac{x}{a}\right)^3\right]dx \quad (10)$$

$$\frac{\partial}{\partial x}\left\{\frac{2}{\sqrt{2\pi(a-x)}}\left[1 + m_1\left(1-\frac{x}{a}\right) + m_2\left(1-\frac{x}{a}\right)^2 + m_3\left(1-\frac{x}{a}\right)^3\right]\right\}\Bigg|_{x=0} = 0 \quad (11)$$

where the efficacy of the last equation (11) (which implies zero slope at crack mouth) is demonstrated by Shen & Glinka [**?**]. They [**?**] compared effect of (11) with that of another condition that curvature of opened crack is zero at the crack mouth, to conclude that this condition (11) leads to more accurate WF. Solving the three equations Eqs. (9)-(11) simultaneously, the unknowns can be obtained as:

$$m_1 = \frac{1}{16}\left[2 + 420\left(\frac{\pi}{\sqrt{2}}F_I^{(r1)} - 2\right) - 315\left(\frac{\pi}{\sqrt{2}}F_I^{(r2)} - \frac{2}{3}\right)\right] \quad (12)$$

$$m_2 = -\frac{7}{12}\left[1 + 105\left(\frac{\pi}{\sqrt{2}}F_I^{(r1)} - 2\right) - 90\left(\frac{\pi}{\sqrt{2}}F_I^{(r2)} - \frac{2}{3}\right)\right] \quad (13)$$

$$m_3 = \frac{21}{80}\left[2 + 120\left(\frac{\pi}{\sqrt{2}}F_I^{(r1)} - 2\right) - 105\left(\frac{\pi}{\sqrt{2}}F_I^{(r2)} - \frac{2}{3}\right)\right] \quad (14)$$

3.2. Universal WF by Glinka and Shen

This universal WF by Glinka has a general form (Eq. (5)) with three unknown parameters that can be determined by solving a system of three equations using the method of two reference SIFs [?]. The unknown coefficients in this case are obtained as:

$$m_1 = \frac{2}{9}\left[2 + 42\left(\frac{\pi}{\sqrt{2}}F_I^{(r1)} - 2\right) - 75\left(\frac{\pi}{\sqrt{2}}F_I^{(r2)} - \frac{2}{3}\right)\right] \tag{15}$$

$$m_2 = -\frac{5}{3}\left[1 + 12\left(\frac{\pi}{\sqrt{2}}F_I^{(r1)} - 2\right) - 24\left(\frac{\pi}{\sqrt{2}}F_I^{(r2)} - \frac{2}{3}\right)\right] \tag{16}$$

$$m_3 = \frac{2}{3}\left[2 + 15\left(\frac{\pi}{\sqrt{2}}F_I^{(r1)} - 2\right) - 30\left(\frac{\pi}{\sqrt{2}}F_I^{(r2)} - \frac{2}{3}\right)\right] \tag{17}$$

Using the Eq. (6) as the WF form, the three unknowns are also determined using the same method of two reference SIFs, and the unknown coefficient for this WF form is obtained as:

$$m_1 = -\frac{5}{104}\left[2 + 90\left(\frac{\pi}{\sqrt{2}}F_I^{(r1)} - 2\right) - 147\left(\frac{\pi}{\sqrt{2}}F_I^{(r2)} - \frac{2}{3}\right)\right] \tag{18}$$

$$m_2 = -\frac{35}{104}\left[14\left(\frac{\pi}{\sqrt{2}}F_I^{(r1)} - 2\right) - 9\left(\frac{\pi}{\sqrt{2}}F_I^{(r2)} - \frac{2}{3}\right) - 2\right] \tag{19}$$

$$m_3 = \frac{3}{13}\left[40\left(\frac{\pi}{\sqrt{2}}F_I^{(r1)} - 2\right) - 35\left(\frac{\pi}{\sqrt{2}}F_I^{(r2)} - \frac{2}{3}\right) - 2\right] \tag{20}$$

3.3. Dual form factor method

In this method, WF form in Eq. (7) is used in which the unknown coefficients are obtained by solving the two integral equations from the two reference configurations as in Eq. (21) & (22).

$$K_I^{r1} = \sigma_0\sqrt{\pi a}F_I^{(r1)} = \int_0^a \sigma_{yy}^{r1}(x)\sqrt{\frac{2}{\pi a}}\left[\left(1 - \frac{x}{a}\right)^{-1/2} + m_1\left(1 - \frac{x}{a}\right)^{1/2} + m_2\left(1 - \frac{x}{a}\right)^{3/2}\right]dx \tag{21}$$

$$K_I^{r2} = \sigma_0\sqrt{\pi a}F_I^{(r2)} = \int_0^a \sigma_{yy}^{r2}(x)\sqrt{\frac{2}{\pi a}}\left[\left(1 - \frac{x}{a}\right)^{-1/2} + m_1\left(1 - \frac{x}{a}\right)^{1/2} + m_2\left(1 - \frac{x}{a}\right)^{3/2}\right]dx \tag{22}$$

Solving the above equations gives the values of m_1 and m_2 as:

$$m_1 = \frac{5}{6}\left(15\sqrt{2}\pi F_I^{(r1)} - 21\sqrt{2}\pi F_I^{(r2)} - 32\right) \tag{23}$$

$$m_2 = -\frac{35}{48}\left(9\sqrt{2}\pi F_I^{(r1)} - 15\sqrt{2}\pi F_I^{(r2)} - 16\right) \tag{24}$$

Similarly, the WF form (WF DFF Form-2) in Eq. (8) is also solved to obtain the unknown coefficients as:

$$m_1 = \frac{15}{4}\left(2\sqrt{2}\pi F_I^{(r1)} - 3\sqrt{2}\pi F_I^{(r2)} - 4\right) \tag{25}$$

$$m_2 = 16 - 9\sqrt{2}\pi F_I^{(r1)} + 15\sqrt{2}\pi F_I^{(r2)} \tag{26}$$

4. Form factors ($F_I^{(r1)}$ & $F_I^{(r2)}$) from reference configurations using FEM

The form factors ($F_I^{(r1)}$ & $F_I^{(r2)}$) in the solutions of unknown coefficients (m_i, expressed in Eqs. (12)-(20), (23)-(26)) in the different WF forms, obtained from the method of two reference SIFs, are obtained by modeling and solving the two loading configurations of uniform and linear crack face pressure using FEM in ABAQUS software. Both inner and outer edge cracked rings are modeled with crack lengths ranging from $0 < a/w < 1$ for different inner to outer radii ratios ((R_i/R_o) varied from 0.1 to 0.9 in steps of 0.1).

Using the symmetry of the problem (for both inner and outer edge cracked rings) along the horizontal and vertical axes that pass through the center, only a quarter of the ring is modeled in ABAQUS. Typical cases of quarter models of the inner and outer edge cracked circular rings are shown in Figs. 4(a) & 5(a) respectively. Both the models are meshed using eight-node CPE8 quadratic elements in ABAQUS. To capture the crack-tip singularity, quarter-point elements are used which are shown in a magnified view in Figs. Figs. 4(b) & 5(b) respectively, for the two ring specimens. The dimensions of the inner/outer cracked circular ring for the finite element models are: outer radius $R_o = 10$ mm, inner radius is varied to get 9 cases as $R_i = 1, 2, \ldots, 9$ mm, thus characteristic width $w = R_o - R_i$ also varies accordingly among the 9 cases. Crack length in each case is varied from 0.1 mm to ($w - 0.1$ mm) in steps of 0.1 mm. For all the cases of FE models, Young's modulus, $E = 200$ GPa, and Poisson's ratio, $\nu = 0.3$ are supplied. The static

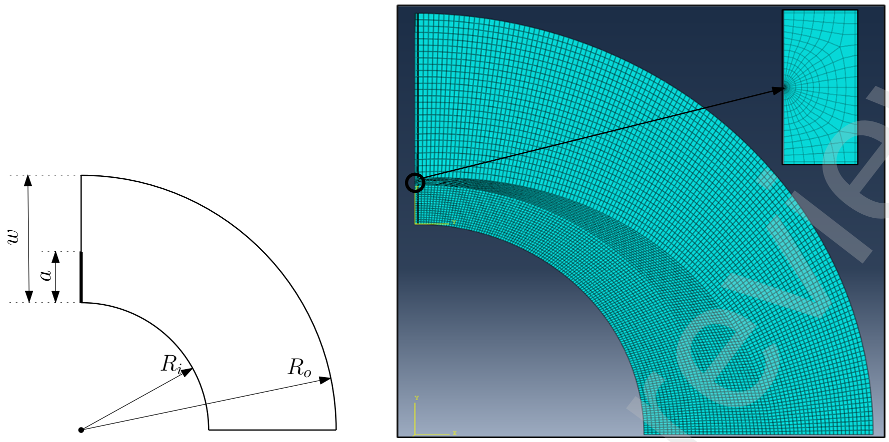

(a) (b)

Figure 4: Inner double edge cracked circular ring ($R_i/R_o = 0.5$ & $a/w = 0.2$): (a) Quarter model of cracked ring (b) Meshed model of cracked ring.

analysis in ABAQUS is done by applying uniform crack face pressure, $\sigma_0 = 1$ MPa, and a linear crack face pressure of maximum load, $\sigma_0 = 1$ MPa on both inner and outer cracked rings. The contour integral technique available in the software is used for defining the cracks and the fracture parameter, K_I is extracted for all the cases. A total of 2×882 cases of the two rings are solved in the software for getting the SIF solutions of the two reference configurations.

4.1. Mesh Insensitivity Analysis

For a typical case of a cracked circular ring of $R_i/R_o = 0.5$, a mesh convergence is tested for both uniform and linear crack face loading configurations. By keeping all other meshing details constant, the number of elements around the crack-tip (n) is varied for various values of s (number of elements along the crack line). A plot of form factor (F_I) for various values of s and n, is shown in Figs. 6(a) & (b), respectively for uniform and linear crack face pressures for inner edge cracked rings and Figs. 6(c) & (d) for outer edge cracked rings.

From Fig. 6, it can be observed that for both the cases of loading configurations, F_I is converging as the n and s increases. For $n > 16$, the curves of F_I become horizontal lines for $s > 8$. From this mesh insensitivity study, it can be concluded that the F_I is converged for $n \geq 20$ and $s \geq 12$. So,

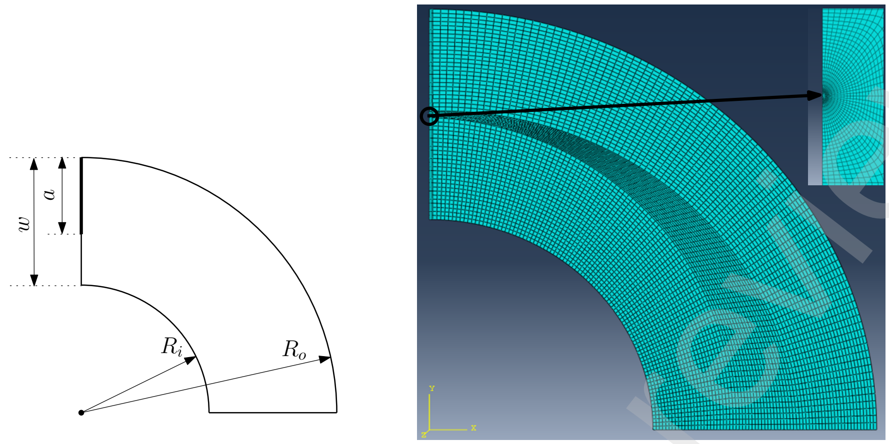

(a) (b)

Figure 5: Outer double edge cracked circular ring ($R_i/R_o = 0.5$ & $a/w = 0.5$): (a) Quarter model of cracked ring (b) Meshed model of cracked ring.

for further analysis of the inner and outer edge cracked rings, the values are taken as $n = 20$ and $s = 12$.

4.1.1. FE solution for F_I for inner/outer cracked rings

The mode-I stress intensity factor (K_I) solutions for all the cases of R_i/R_o for various crack length ratios (a/w) for the two reference configurations (uniform and linear crack-face pressure) obtained from FE simulations in Abaqus software are then normalized using Eq. (27) to get the form factors (F_I).

$$F_I = \frac{K_I}{\sigma_0\sqrt{\pi a}} \tag{27}$$

The form factors thus obtained for the various R_i/R_o and a/w are then curve fitted to use in the WF derivation as mentioned in Section 3. A polynomial equation in a/w is used to fit the F_I for the two cases of loading configurations. The singularity of the form factor at the boundary is captured by introducing a term $(1 - a/w)^{3/2}$ into the polynomial function for all the cases. Thus, the form factors obtained for the uniform and linear crack-face pressures for different R_i/R_o are fitted using the Eqs. (28) & (29) respectively.

$$F_I^{(r1)} = \frac{K_I^{(r1)}}{\sigma_0\sqrt{\pi a}} = \frac{1}{\left(1 - \frac{a}{w}\right)^{3/2}} \sum_{i=0}^{6} A_i \left(\frac{a}{w}\right)^i \tag{28}$$

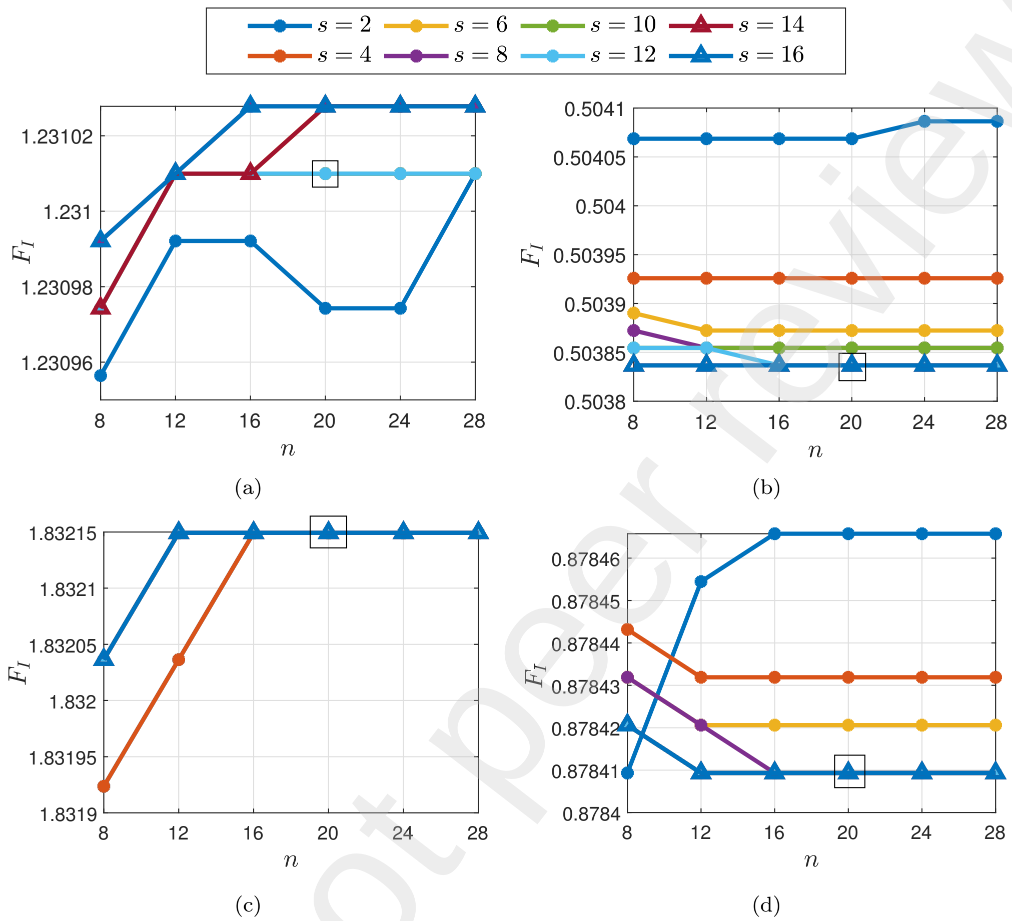

Figure 6: Mesh Insensitivity: Normalized SIF (F_I) versus n (Number of elements around crack-tip) for various s (number of divisions along the crack-line): (a & b) Inner edge cracked ring (c & d) Outer edge cracked ring (a & c) Uniform crack-face pressure and (b & d) Linear distribution of crack-face pressure.

$$F_I^{(r2)} = \frac{K_I^{(r2)}}{\sigma_0\sqrt{\pi a}} = \frac{1}{\left(1-\frac{a}{w}\right)^{3/2}} \sum_{i=0}^{6} B_i \left(\frac{a}{w}\right)^i \tag{29}$$

The curve fitting is done using the MATLAB software. The coefficients A_i for $F_I^{(r1)}$ (uniform crack face pressure) and B_i for $F_I^{(r2)}$ (linear crack face pressure) are obtained for inner edge cracked double edge cracked circular rings of various R_i/R_o, which is tabulated and presented in Table 1.

Similarly, the form factors for the outer double edge cracked circular ring specimen are also curve fitted using Eqs. (28) & (29), respectively for

Table 1: Coefficients (A_i & B_i) for $F_I^{(r1)}$ and $F_I^{(r2)}$ for WF of inner double edge cracked circular ring specimens

R_i/R_o	A_0 B_0	A_1 B_1	A_2 B_2	A_3 B_3	A_4 B_4	A_5 B_5	A_6 B_6
0.1	1.036 0.3862	−2.359 −1.094	7.713 4.697	−19.16 −11.88	25.16 15.52	−17.26 −10.63	4.871 2.997
0.2	1.078 0.4128	−2.477 −1.167	7.981 4.868	−19.21 −11.9	24.35 14.99	−16.25 −9.992	4.523 2.781
0.3	1.095 0.4229	−2.242 −1.022	6.79 4.132	−15.97 −9.867	19.46 11.92	−12.69 −7.78	3.559 2.191
0.4	1.101 0.4268	−1.984 −0.863	5.745 3.475	−13.06 −8.006	14.82 8.976	−9.295 −5.663	2.673 1.654
0.5	1.103 0.428	−1.742 −0.7134	4.784 2.87	−9.95 −6.041	9.674 5.785	−5.719 −3.52	1.85 1.191
0.6	1.102 0.4275	−1.513 −0.5751	3.855 2.315	−6.851 −4.224	5.266 3.358	−3.649 −2.601	1.79 1.3
0.7	1.104 0.4298	−1.468 −0.5657	4.502 2.868	−9.975 −6.765	13.51 9.695	−13.69 −9.977	6.011 4.317
0.8	1.142 0.4552	−2.392 −1.195	13.05 8.617	−41.89 −28.2	73.71 50.01	−68.3 −46.42	24.69 16.74
0.9	1.167 0.4699	−2.656 −1.317	14.51 9.099	−43.88 −27.72	73.15 46.29	−62.67 −39.64	20.2 12.69

Table 2: Coefficients (A_i & B_i) for $F_I^{(r1)}$ and $F_I^{(r2)}$ for WF of outer double edge cracked circular ring specimens

R_i/R_o	A_0 B_0	A_1 B_1	A_2 B_2	A_3 B_3	A_4 B_4	A_5 B_5	A_6 B_6
0.1	1.114 0.4356	−0.6962 −0.101	−2.397 −1.201	4.833 1.839	−6.823 −2.554	6.199 2.62	−2.228 −1.038
0.2	1.116 0.437	−0.8513 −0.1945	−1.255 −0.5173	2.517 0.4464	−4.762 −1.24	5.29 1.928	−2.053 −0.859
0.3	1.118 0.4378	−0.9881 −0.2651	−0.1331 0.05102	0.3557 −0.4727	−2.9 −0.7083	4.262 1.711	−1.714 −0.7539
0.4	1.117 0.4369	−1.03 −0.2801	0.2656 0.1929	0.7407 0.1133	−5.079 −2.557	6.101 3.172	−2.115 −1.077
0.5	1.113 0.4341	−0.9806 −0.2422	−0.003006 −0.04322	3.239 1.87	−10.14 −5.936	9.59 5.43	−2.814 −1.512
0.6	1.107 0.4305	−0.8909 −0.1891	−0.4208 −0.2923	5.635 3.275	−13.65 −7.835	10.65 5.747	−2.429 −1.136
0.7	1.107 0.4313	−1.013 −0.2856	1.219 0.8933	−0.3773 −1.114	−0.5275 1.604	−3.603 −4.289	3.197 2.761
0.8	1.147 0.4585	−2.204 −1.086	11.72 7.88	−38.63 −26.53	70.09 48.43	−66.58 −45.92	24.46 16.77
0.9	1.172 0.473	−2.62 −1.29	14.17 8.87	−43.12 −27.22	72.46 45.83	−62.4 −39.43	20.15 12.64

uniform and linear crack face pressures of various R_i/R_o, which is tabulated in Table 2.

5. Results and Discussion

5.1. Testing various WF forms used for finding SIFs in double edge cracked rings

The various forms of WF as in Eqs. (3), (5), (6), (7), & (8) is used here to determine the SIFs in double edge (inner/outer) cracked rings subjected to a quadratic crack face pressure ($n = 2$ in Eq. (30)) and a cubic crack face pressure ($n = 3$ in Eq. (30)). The coefficients (m_i) in the WF forms are determined using the two reference form factors, which are tabulated in Tables 1 & 2, respectively for inner and outer cracked rings. The form factor results obtained from WF forms are then compared with that obtained from FEM using ABAQUS for the same two loading cases.

$$\sigma_{yy}(x) = \sigma_0 \left(1 - \frac{x}{a}\right)^n \quad ; \quad n = 2 \text{ \& } 3 \tag{30}$$

The F_I obtained for an inner edge cracked ring of R_i/R_o using the WF forms and by FEM, for both quadratic and cubic crack face pressure cases are plotted in Figs. 7(a) & (b) respectively. From the figure it can be observed that F_I curves of different WF forms have errors compared to the FEM results. Note that F_I results from the WF form of Fett have the highest error among the cases considered; thus, such a form is not recommended here for any cracked ring specimens. Compared among other forms, the results of DFF match almost perfectly with those of FEM.

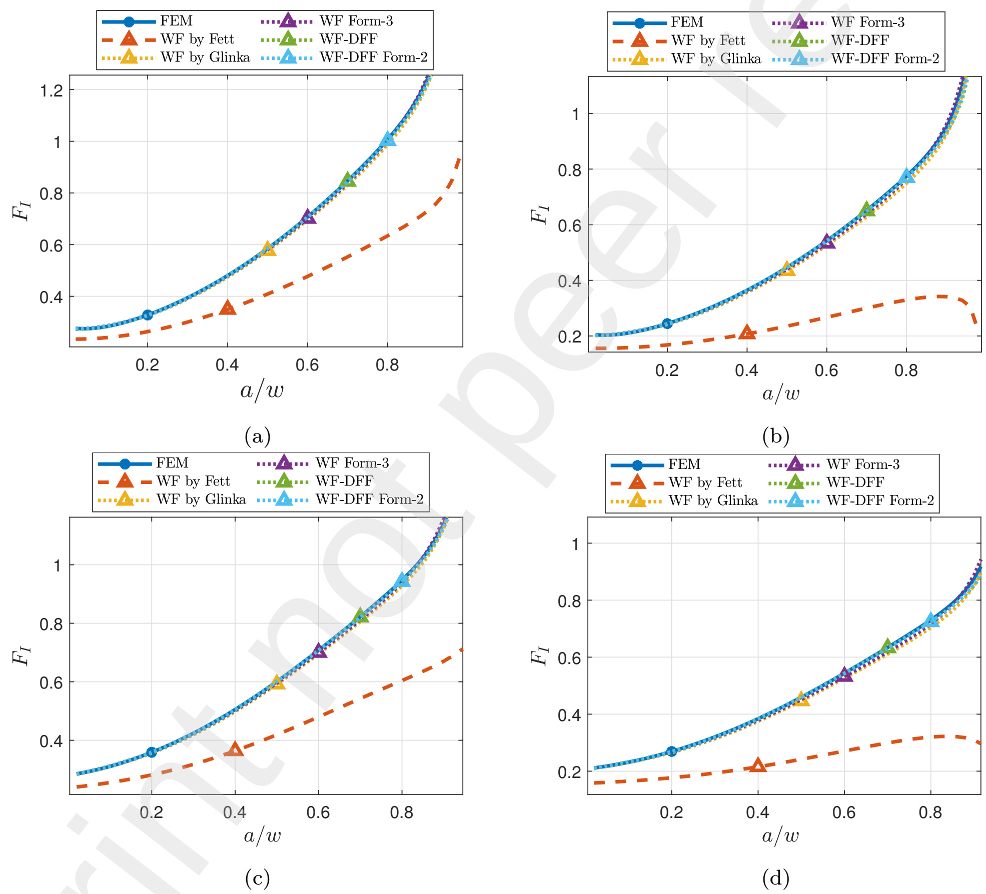

Figure 7: Form factors using WFs and FEM for circular rings of $R_i/R_o = 0.5$ with (a & b) inner double edge cracks & (c & d) outer double edge cracks for (a & c) quadratic & (b & d) cubic crack-face pressures.

The errors in calculating the F_I using the different WF forms are calculated using Eq. (31) for quadratic and cubic crack face pressures in both inner and outer edge cracked rings and are plotted in Fig. 8.

$$Error\ \% = \frac{F_I^{WF} - F_I^{FEM}}{F_I^{FEM}} \times 100\% \tag{31}$$

The error in determining F_I using the WF form by Fett is having error greater than 10%, which is not included in the Fig. 8. From the figure, it can be observed that the error plots for all other forms of WF are having the same trend with a/w, with an overall percentage error less than 5%. Also, for the case of WF forms of DFF and DFF Form-2, the percentage error is less than 1% for both cases of loading (quadratic and cubic crack face pressure) in both inner (Figs. 8(a) & (b)) and outer (Figs. 8(c) & (d)) double edge cracked rings. To understand the errors in finding the F_I using the different WF forms, the root mean square error (RMSE) for each case of the ring specimens is calculated and tabulated in Table 3. From the RMSE values for each WF form, it can be seen that the WF DFF has minimum value for all cases. The next is DFF Form-2 while WF Form-3 takes third place. The general WF of Fett has the highest RMSE value, and the universal WF by Glinka & Shen has the second highest RMSE value for all cases of cracked rings. This error may be attributed to the use of zero slope condition 11 at the crack mouth, as such a condition is not used in DFF and DFF-2 methods which yield accurate WF. Although these two WF forms are applicable in many other crack geometries (central, single, and double edge cracks in finite-width plate [?], radial cracks emanating from bore hole in an infinite plane [? ?]), for the case of circular ring specimens, they are not recommendable. It can be concluded that the WF form of DFF method is recommended here for the inner/outer double edge cracked circular rings for finding the SIFs, as it was used for edge cracked semi disk [?].

The COD-based weight function for the two ring specimens derived by Wu & Xu [?] is also used to predict F_I for quadratic and cubic crack-face loadings. The corresponding results are not shown here for brevity. When these predictions are compared with those of the five forms presented in this paper for accuracy, the COD-based WF ranks third after DFF and DFF Form-2. This observation suggests that for ring specimens, DFF or DFF Form-2 based WF works better than all other forms, including the COD-based WF.

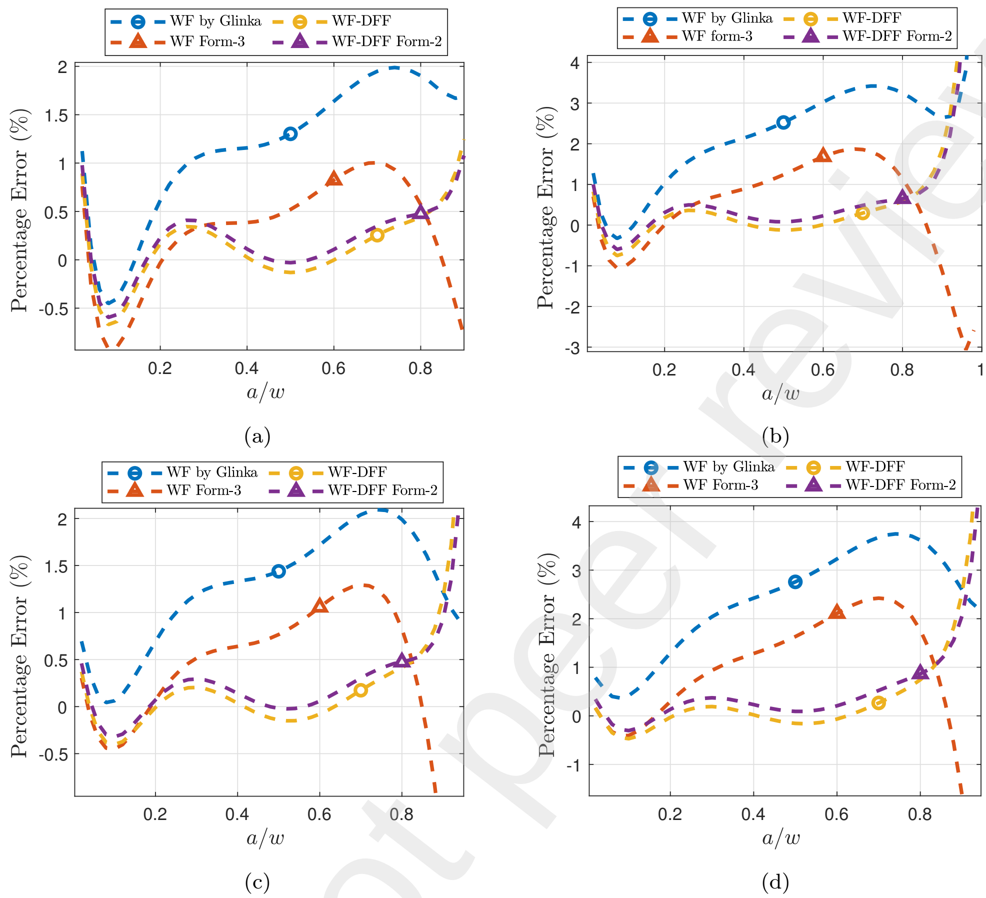

Figure 8: Percentage error in F_I calculation using the four WF forms for circular rings of $R_i/R_o = 0.5$ with (a & b) inner double edge cracks & (c & d) outer double edge cracks for (a & c) quadratic & (b & d) cubic crack-face pressures.

5.2. *Application of the derived WFs to determine SIFs*

The above derived WF of the form in DFF method is used here to determine F_I for both the inner and outer edge cracked rings subjected to uniform compression as shown in Figs. 9 (a) & (b) respectively. The form factors are determined here for both ring specimens by changing their inner to outer radii ratios (R_i/R_o) and the load distribution angle (β) for various crack length ratios (a/w). Four values of R_i/R_o (viz. 0.2, 0.3, 0.5 & 0.7) and six values for β (viz. $0.5°$, $1°$, $2°$, $5°$, $10°$ & $20°$) are considered here for inner/outer ring specimens under uniform compression. The final equation for finding SIF for the inner/outer double edge cracked ring specimen using

Table 3: RMSE for different WF forms for inner and outer edge cracked rings

	RMSE			
	Inner edge cracked ring		Outer edge cracked ring	
WF forms	Quadratic	Cubic	Quadratic	Cubic
1. WF by Fett	0.1971	0.2356	0.1932	0.2314
2. WF by Glinka	0.00101	0.0137	0.0105	0.0148
3. WF Form-3	0.0046	0.0068	0.0060	0.0090
4. WF DFF	0.0016	0.0015	0.0013	0.0016
5. WF DFF-2	0.0019	0.0020	0.0017	0.0022

the WF DFF form is given in Eq. (32).

$$\begin{aligned} K_I = \sigma_0\sqrt{\pi a}F_I = \int_0^a \sigma_{yy}(x)\sqrt{\frac{2}{\pi a}}\Bigg[\left(1-\frac{x}{a}\right)^{-1/2} \\ +\frac{5}{6}\left(15\sqrt{2}\pi F_I^{(r1)} - 21\sqrt{2}\pi F_I^{(r2)} - 32\right)\left(1-\frac{x}{a}\right)^{1/2} \\ -\frac{35}{48}\left(9\sqrt{2}\pi F_I^{(r1)} - 15\sqrt{2}\pi F_I^{(r2)} - 16\right)\left(1-\frac{x}{a}\right)^{3/2}\Bigg]dx \end{aligned} \quad (32)$$

To use Eq. (32), the stress distribution along the prospected crack line ($\sigma_{yy}(x)$) in the uncracked ring geometry is required. This can be obtained from the elasticity solution for a circular ring under diametral compression. Michell series solution can be used here to solve this problem of circular rung under diametral compression which is explained in Appendix A. A circular ring subjected to uniform pressure of $\sigma_0 = P/(\pi R_o h)$ on the outer boundary is considered with total load $P = 150$ N. The geometric dimensions of the ring are chosen as $R_o = 0.1$ m, $R_i = 0.02$, 0.03, 0.05 & 0.07 m and uniform into-the-plane thickness, $h = 0.006$ m.

5.2.1. F_I for an inner double edge cracked circular ring under diametral compression

The mode-I form factors of inner double edge cracked circular ring under diametral compression are determined as per Eq. (32) adopting forms given in Eqs. (28) & (29) with the corresponding coefficients from Table 1 for $F_I^{(r1)}$ and $F_I^{(r2)}$. The stress distribution required from the uncracked geometry is also obtained for use in the SIF equation (Eq. (32)). Then the F_I for different crack length ratios ($a/w = 0.1$ to 0.7) is obtained for the inner

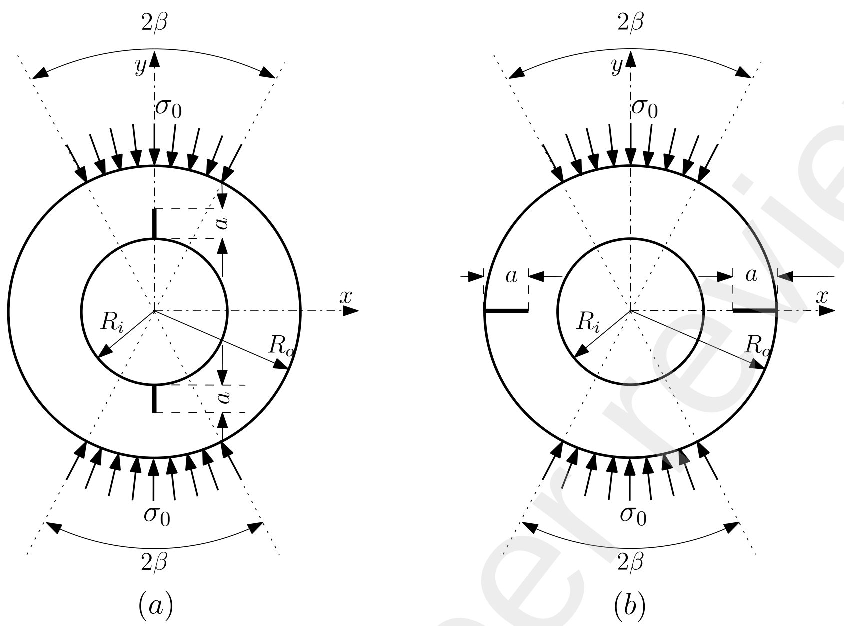

Figure 9: Double edge cracked circular rings at (a) Inner and (b) outer edge under uniform compression on the outer boundary

double edge cracked rings subjected to uniform compression on the outer boundary distributed over various β values $(0.5°, 1°, 2°, 5°, 10°$ and $20°)$ for different R_i/R_o (0.2, 0.3, 0.5 and 0.7) are determined and plotted in Fig. 10.

From Fig. 10, it can be observed that for each case of R_i/R_o in subplots, F_I increases with increasing pressure distribution angle, β. Also, with increasing R_i/R_o, F_I increases. A constant F_I region can be observed for $\beta < 5°$, of the inner double edge cracked circular rings for all R_i/R_o as is the case with edge cracked semi disk under compression [**?**].

5.2.2. F_I for an outer double edge cracked circular ring under daimetral compression

The mode-I form factors of outer double edge cracked circular ring under diametral compression are determined using Eq. (32) and Eqs. (28) & (29) with the corresponding coefficients given in Table 2. The required stresses in the uncracked ring specimen are also obtained. Then the form factors F_I are obtained for different a/w for circular rings of various R_i/R_o with different β values, which are plotted as shown in Fig. 11.

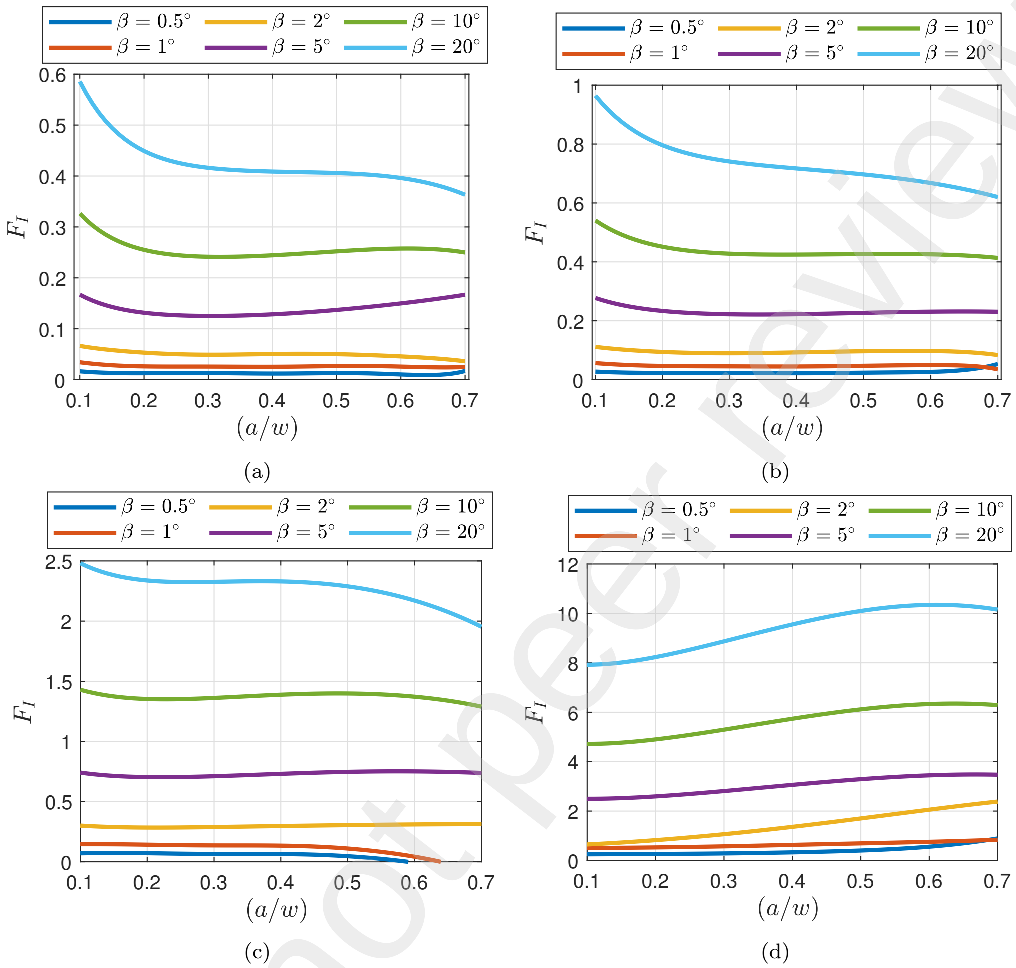

Figure 10: Normalized SIF (F_I) (using WF DFF) in inner double edge cracked circular rings of (a) $R_i/R_0 = 0.2$, (b) $R_i/R_0 = 0.3$, (c) $R_i/R_0 = 0.5$ & (d) $R_i/R_0 = 0.7$ under uniform compression for various β at different a/w values.

From Fig. 11, it can be observed that for outer edge cracked rings with $R_i/R_o = 0.2$ & 0.3, F_I becomes zero and then negative after some a/w. For $R_i/R_o = 0.2$, this transition from positive to negative occurs at $a/w \approx 0.3$, while it occurs at $a/w \approx 0.5$ for $R_i/R_o = 0.3$. Overall the F_I curves resemble normal stress distribution on a section due to bending load caused by pair of moments. This also implies crack closure phenomena when the crack-tip reaches a point where $F_I = 0$ as presented by Iung & Pineau [**?**].

This trend of transition from positive to negative is not observed for

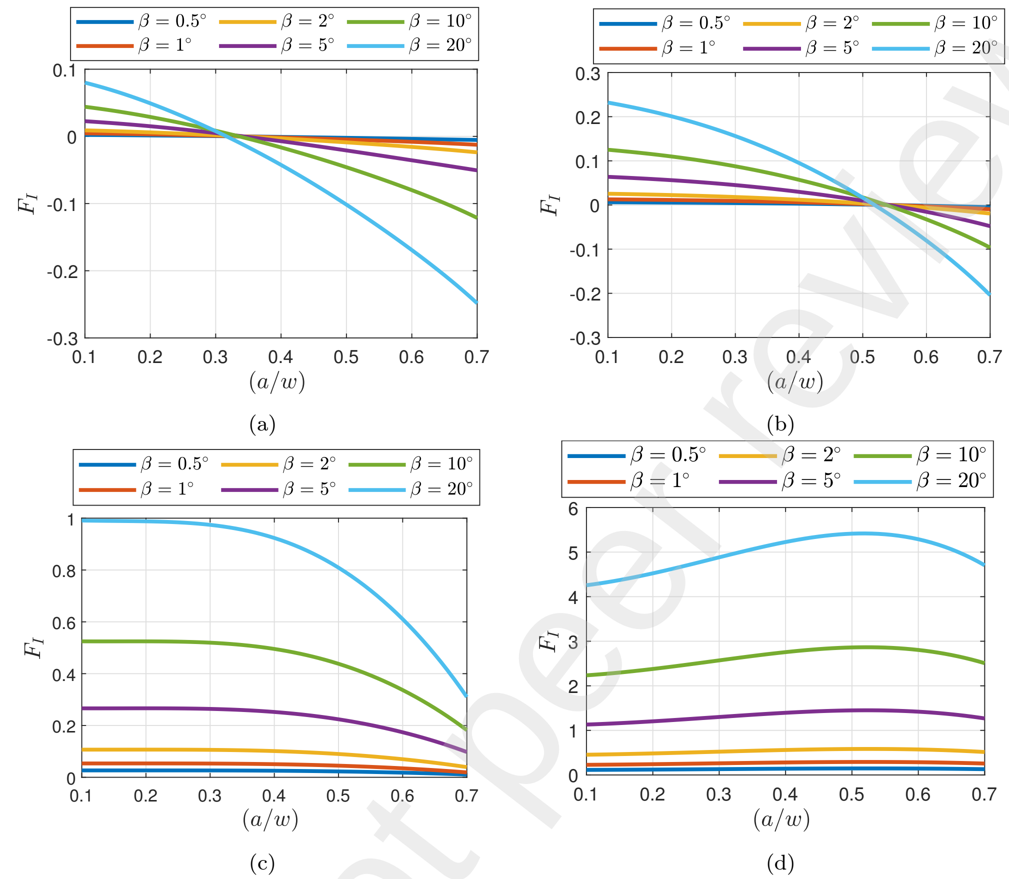

Figure 11: Normalized SIF (F_I) (using WF DFF) in outer double edge cracked circular rings of (a) $R_i/R_0 = 0.2$, (b) $R_i/R_0 = 0.3$, (c) $R_i/R_0 = 0.5$ & (d) $R_i/R_0 = 0.7$ under uniform compression for various β at different a/w values.

$R_i/R_o \geq 0.5$. For cases $R_i/R_o \geq 0.5$, similar to inner edge cracks, the outer edge cracks also show a constant F_I for $\beta < 5°$.

6. Conclusions

Weight functions (WF) are derived to find the mode-I stress intensity factors of inner/outer double edge cracked circular rings for various ratios of inner to outer radii. An investigation is carried out to find the best form of WF from various general and other forms of WF that use the method of two reference stress intensity factors (SIFs). The derived WF is then applied to find SIFs in two different types of crack face loading to test the accuracy by comparing the results using FEM. Three forms from the literature and two other derived forms are compared, which resulted in the conclusion that the dual form factor form gives the best results for the circular ring specimens. The percentage error obtained for the dual form factor (DFF) method is less than 1%. In addition, the RMSE (root mean square error) value is also the least value for this method. The form factors in the inner/outer double edge cracked circular ring subjected to uniform compression with different contact angles (β) are then determined using the DFF WF method. The form factors are found to depend on β for all R_i/R_o.

Appendix A. Elasticity solution for an uncracked circular ring under diametral compression

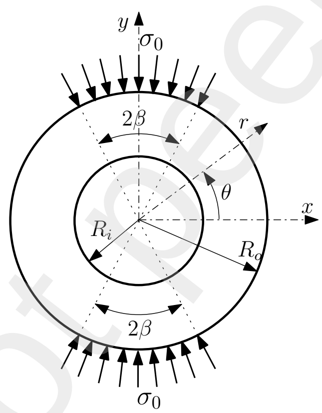

Figure A.12: Circular ring under uniform compression on the outer boundary.

A circular ring under diametral compression as in Fig. A.12 is solved using the Michell generalised series solution method [**?**]. A ring of inner radius R_i, outer radius R_o and thickness h, which is loaded by a total load of P are considered. A coordinate system is assumed at the centre of the ring with x-axis as the horizontal and y-axis as the vertical axis. A homogeneous, linear -elastic isotropic material under plane state of stress is considered here for the problem. The boundary conditions are: Symmetry about x and y axes:

$$\begin{aligned} u_\theta(r, \theta = 0) &= u_\theta(r, \theta = \pi/2) = 0 \\ \Longrightarrow \tau_{r\theta}(r, \theta = 0) &= \tau_{r\theta}(r, \theta = \pi/2) = 0 \end{aligned} \tag{A.1}$$

and other boundary conditions include:

$$\sigma_{rr}(r = R_i, \theta) = \tau_{r\theta}(r = R_i, \theta) = \tau_{r\theta}(r = R_o, \theta) = 0$$
$$\sigma_{rr}(r = R_o, \theta) = \sigma_0, \text{when}(\pi/2 - \beta) \leq \theta \leq \pi/2 \text{ and zero elsewhere.} \quad \text{(A.2)}$$

where, σ_{rr} and $\tau_{r\theta}$ are the normal and shear stress components, β is the half loading angle.

The stress components obtained from the generalized solution of biharmonic equation by Michell in polar coordinates can be given as:

$$\begin{aligned}\sigma_{rr} =& 2b_o + \frac{c_1'}{r^2} - \sum_{n=2}^{\infty} \big\{ n(n-1)a_n r^{n-2} + (n+1)(n-2)b_n r^n \\ &+ n(n+1)c_n r^{-n-2} + (n+2)(n-1)d_n r^{-n} \big\} \cos n\theta \end{aligned} \quad \text{(A.3)}$$

$$\begin{aligned}\sigma_{\theta\theta} =& 2b_o - \frac{c_1'}{r^2} + \sum_{n=2}^{\infty} \big\{ n(n-1)a_n r^{n-2} + (n+1)(n+2)b_n r^n \\ &+ n(n+1)c_n r^{-n-2} + (n-2)(n-1)d_n r^{-n} \big\} \cos n\theta \end{aligned} \quad \text{(A.4)}$$

$$\begin{aligned}\tau_{r\theta} =& \sum_{n=2}^{\infty} n \big\{ (n-1)a_n r^{n-2} + (n+1)b_n r^n \\ &- (n+1)c_n r^{-n-2} - (n-1)d_n r^{-n} \big\} \sin n\theta \end{aligned} \quad \text{(A.5)}$$

The unknown coefficients (a_n, b_n, c_n, d_n, c_1' & b_0) of truncated series in the above equations are obtained by solving the simultaneous linear equations formulated using the boundary conditions given in Eqs. (A.1) & (A.2), by expressing the boundary tractions in terms of Fourier series'.